

# Curvature and scaling in 4D dynamical triangulation

Bas V. de Bakker\*

Jan Smit†

Institute for Theoretical Physics, University of Amsterdam  
Valckenierstraat 65, 1018 XE Amsterdam, the Netherlands.

12 December 1994

## Abstract

We study the average number of simplices  $N'(r)$  at geodesic distance  $r$  in the dynamical triangulation model of euclidean quantum gravity in four dimensions. We use  $N'(r)$  to explore definitions of curvature and of effective global dimension. An effective curvature  $R_V$  goes from negative values for low  $\kappa_2$  (the inverse bare Newton constant) to slightly positive values around the transition  $\kappa_2^c$ . Far above the transition  $R_V$  is hard to compute. This  $R_V$  depends on the distance scale involved and we therefore investigate a similar explicitly  $r$  dependent ‘running’ curvature  $R_{\text{eff}}(r)$ . This increases from values of order  $R_V$  at intermediate distances to very high values at short distances. A global dimension  $d$  goes from high values in the region with low  $\kappa_2$  to  $d = 2$  at high  $\kappa_2$ . At the transition  $d$  is consistent with 4. We present evidence for scaling of  $N'(r)$  and introduce a scaling dimension  $d_s$  which turns out to be approximately 4 in both weak and strong coupling regions. We discuss possible implications of the results, the emergence of classical euclidean spacetime and a possible ‘triviality’ of the theory.

---

\*email: bas@phys.uva.nl

†email: jsmit@phys.uva.nl

# 1 Introduction

The dynamical triangulation model [1, 2, 3] is a very interesting candidate for a nonperturbative formulation of four-dimensional euclidean quantum gravity. The configurations in the model are obtained by glueing together equilateral four-dimensional simplices in all possible ways such that a simplicial manifold is obtained. A formulation using hypercubes was pioneered in [4]. The simplicial model with spherical topology is defined as a sum over triangulations  $\mathcal{T}$  with the topology of the hypersphere  $S^4$  where all the edges have the same length  $\ell$ . The partition function of this model is

$$Z(N, \kappa_2) = \sum_{\mathcal{T}, N_4=N} \exp(\kappa_2 N_2). \quad (1)$$

Here  $N_i$  is the number of simplices of dimension  $i$  in the triangulation  $\mathcal{T}$ . The weight  $\exp(\kappa_2 N_2)$  is part of the Regge form of the Einstein-Hilbert action  $-\int \sqrt{g}R/16\pi G_0$ ,

$$-S = \frac{1}{16\pi G_0} \sum_{\Delta} V_2 2\delta_{\Delta} = \kappa_2(N_2 - \rho N_4), \quad (2)$$

$$\kappa_2 = \frac{V_2}{8G_0}, \quad \rho = \frac{10 \arccos(1/4)}{2\pi} = 2.098 \dots, \quad (3)$$

Here  $V_2$  is the volume of 2-simplices (triangles  $\Delta$ ) and  $\delta_{\Delta}$  is the deficit angle around  $\Delta$ . The volume of an  $i$ -simplex is

$$V_i = \ell^i \sqrt{(i+1)/2^i/i!}. \quad (4)$$

Because the  $N_i$  ( $i = 0 \dots 4$ ) satisfy three constraints only two of them are independent. We have chosen  $N_2$  and  $N_4$  as the independent variables. For comparison with other work we remark that if  $N_0$  is chosen instead of  $N_2$  then the corresponding coupling constant  $\kappa_0$  is related to  $\kappa_2$  by  $\kappa_0 = 2\kappa_2$ . This follows from the relations between the  $N_i$ , which imply that

$$N_0 - \frac{1}{2}N_2 + N_4 = \chi, \quad (5)$$

where  $\chi$  is the Euler number of the manifold, which is 2 for  $S^4$ .

Average values corresponding to (1) can be estimated by Monte Carlo methods, which require varying  $N_4$  [1, 2, 3]. One way to implement the condition  $N_4 = N$  is to base the simulation on the partition function [1]

$$Z'(N, \kappa_2) = \sum_{\mathcal{T}} \exp(\kappa_2 N_2 - \kappa_4 N_4 - \gamma(N_4 - N)^2), \quad (6)$$

where  $\kappa_4$  is chosen such that  $\langle N_4 \rangle \approx N$  and the parameter  $\gamma$  controls the volume fluctuations. The precise values of these parameters are irrelevant if the desired  $N_4$  are picked from the ensemble described by (6). This is not done in practice but the results are insensitive to reasonable variations in  $\gamma$ . We have chosen the parameter  $\gamma$  to be  $5 \cdot 10^{-4}$ , giving  $\langle N_4^2 \rangle - \langle N_4 \rangle^2 \approx (2\gamma)^{-1} = 1000$ , i.e. the fluctuations in  $N_4$  are approximately 30.

Numerical simulations [1, 2, 3, 5, 6, 7, 8] have shown that the system (6) can be in two phases\*. For  $\kappa_2 > \kappa_2^c(N_4)$  (weak bare coupling  $G_0$ ) the system is in an elongated phase with high  $\langle \bar{R} \rangle$ , where  $\langle \bar{R} \rangle$  is the average Regge curvature

$$\bar{R} = \frac{2\pi V_2}{V_4} \left( \frac{N_2}{N_4} - \rho \right) \longleftrightarrow \frac{\int \sqrt{g} R}{\int \sqrt{g}}. \quad (7)$$

In this phase the system has relatively large baby universes [9] and resembles a branched polymer. For  $\kappa_2 < \kappa_2^c(N_4)$  (strong coupling) the system is in a crumpled phase with low  $\langle \bar{R} \rangle$ . This phase is highly connected, i.e. the average number of simplices around a point is very large. The transition between the phases appears to be continuous.

As an example and for later reference we show in figure 1 the susceptibility

$$\left[ \left\langle \left( \frac{N_2}{N_4} \right)^2 \right\rangle - \left\langle \frac{N_2}{N_4} \right\rangle^2 \right] N = \frac{V_4}{(2\pi V_2)^2} \left[ \langle \bar{R}^2 \rangle - \langle \bar{R} \rangle^2 \right] V. \quad (8)$$

( $V = N_4 V_4$ ). The two curves are for  $N = 8000$  and 16000 simplices.

The data for  $N = 8000$  are consistent with those published in reference [8], where results are given for

$$\chi(N_0) = \frac{1}{N} \left( \langle N_0^2 \rangle - \langle N_0 \rangle^2 \right). \quad (9)$$

---

\*In section 6 we discuss the possibility that these are not phases in the sense of conventional statistical mechanics.

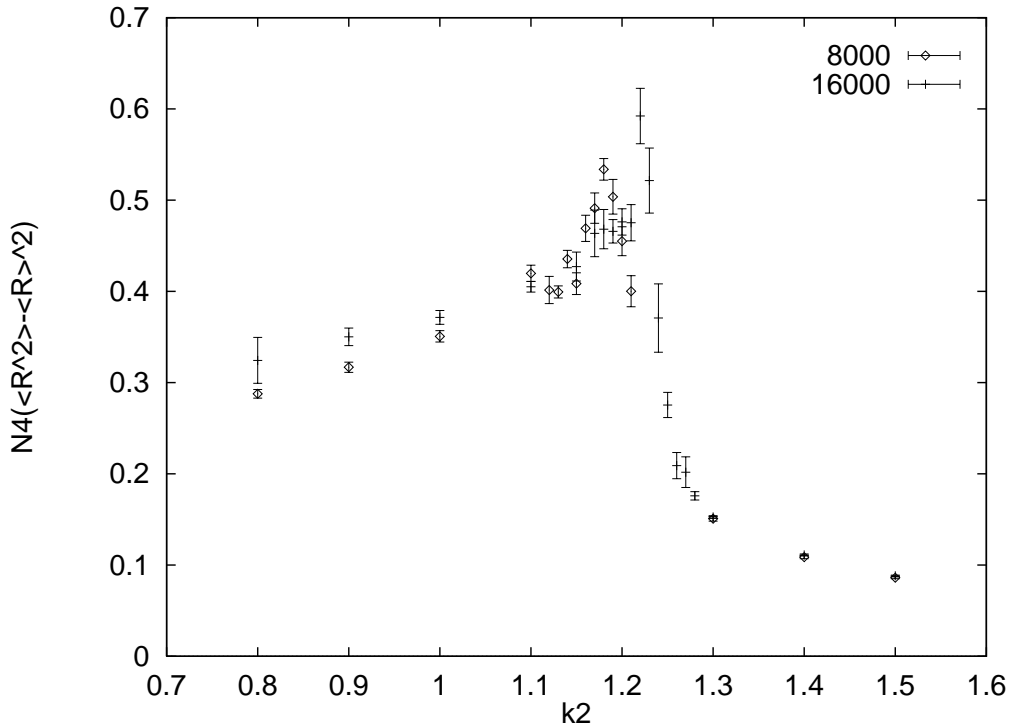


Figure 1: The curvature susceptibility as a function of  $\kappa_2$  for 8000 and 16000 simplices.

For fixed  $N_4$  this is 1/4 of our curvature susceptibility (8), as can be seen from (5).

The behavior of  $Z(\kappa_2, N)$  as a function of  $N$  for large  $N$  has been the subject of recent investigations [10, 11, 13, 12]. In ref. [13] we discussed the possibility that  $\kappa_2^c$  might move to infinity as  $N \rightarrow \infty$  and argued that this need not invalidate the model. So far a finite limit is favoured by the data [11, 12], however.

It is of course desirable to get a good understanding of the properties of the euclidean spacetimes described by the probability distribution  $\exp(-S)$ . A very interesting aspect is the proliferation of baby universes [9]. Here we study more classical aspects like curvature and dimension, extending previous work in this direction [1, 2, 3, 5, 6, 7, 8]. The basic observable for this purpose is the average number of simplices at a given geodesic distance from the

$\kappa_2$	8000	16000
0.80	29	16
0.90	34	19
1.00	38	25
1.10	37	38
1.12	13	–
1.13	24	–
1.14	28	–
1.15	21	13
1.16	36	–
1.17	44	16
1.18	90	8
1.19	26	22

$\kappa_2$	8000	16000
1.20	56	45
1.21	22	56
1.22	–	51
1.23	–	65
1.24	–	58
1.25	–	45
1.26	–	38
1.27	–	31
1.28	–	43
1.30	43	41
1.40	40	24
1.50	47	21

Table 1: Number of configurations used in the various calculations.

arbitrary origin,  $N'(r)$ . We want to see if this quantity can be characterized, approximately, by classical properties like curvature and dimension, and if for suitable bare couplings  $\kappa_2$  there is a regime of distances where the volume-distance relation  $N'(r)$  can be given a classical interpretation. It is of course crucial for such a continuum interpretation of  $N'(r)$  that it scales in an appropriate way.

In section 2 we investigate the properties of an effective curvature for a distance scale that is large compared to the basic unit but small compared to global distances. Effective dimensions for global distances are the subject of section 3 and scaling is investigated in section 4. We summarize our results in section 5 and discuss the possible implications in section 6.

## 2 Curvature

A straightforward measure of the average local curvature is the bare curvature at the triangles, i.e.  $\langle \bar{R} \rangle = 48\pi\sqrt{3/5}\ell^{-2}\langle N_2/N_4 - \rho \rangle$  (this follows from (7) and (4)). It has been well established that at the phase transition  $\langle N_2/N_4 - \rho \rangle \approx 2.38 - 2.10 = 0.28$ , practically independent of the volume [1, 2, 3, 5]. This means that  $\langle \bar{R} \rangle \approx 55\ell^{-2}$  has to be divergent in the continuum limit  $\ell \rightarrow 0$ . However, the curvature at scales large compared to the lattice distance  $\ell$  is

not necessarily related to the average curvature at the triangles. One could imagine e.g. a spacetime with highly curved baby universes which is flat at large scales.

The scalar curvature at a point is related to the volume of a small hypersphere around that point. Expanding the volume in terms of the radius of the hypersphere results in the relation

$$V(r) = C_n r^n \left(1 - \frac{R_V r^2}{6(n+2)} + O(r^4)\right), \quad (10)$$

$$C_n = \frac{\pi^{n/2}}{\Gamma(n/2 + 1)}, \quad (11)$$

for an  $n$ -dimensional manifold. We have written  $R_V$  here to distinguish it from the small scale curvature at the triangles. Differentiating with respect to  $r$  results in the volume of a shell at distance  $r$  with width  $dr$ ,

$$V'(r) = C_n n r^{n-1} \left(1 - \frac{R_V r^2}{6n} + O(r^4)\right). \quad (12)$$

We explore this definition of curvature as follows. We take the dimension  $n = 4$ , assuming that there is no need for a fractional dimension differing from 4 at small scales. For  $r$  we take the geodesic distance between the simplices, that is the lowest number of hops from four-simplex to neighbour needed to get from one four-simplex to the other. Setting the distance between the centers of neighbouring simplices to 1 corresponds to taking a fixed edge length in the simplicial complex of  $\sqrt{10}$ , i.e. we will use lattice units with  $\ell = \sqrt{10}$ . For  $V(r)$  and  $V'(r)$  we take

$$V(r) = V_{\text{eff}} N(r), \quad V'(r) = V_{\text{eff}} N'(r), \quad N'(r) = N(r) - N(r-1), \quad (13)$$

where  $N(r)$  is the average number of four-simplices within distance  $r$  from the (arbitrary) origin,  $N'(r)$  is the number of simplices at distance  $r$  and we have allowed for an effective volume  $V_{\text{eff}}$  per simplex which is different from  $V_4$ . Since  $R_V$  is to be a long distance (in lattice units) observable we shall call it the effective curvature.

The effective curvature was determined by fitting the function  $N'(r)$  to

$$N'(r) = ar^3 + br^5. \quad (14)$$

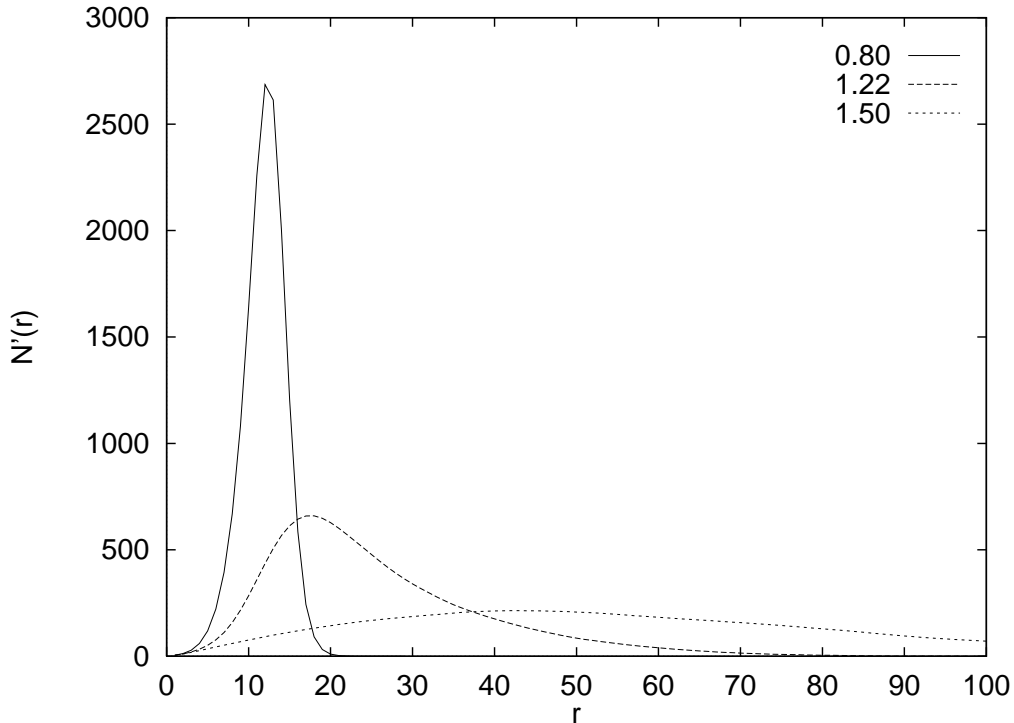


Figure 2: The number of simplices  $N'(r)$  at distance  $r$  from the origin at  $\kappa_2 = 0.80, 1.22$  and  $1.50$ , for  $N = 16000$ .

It then follows from (12) and (13) that  $R_V$  and  $V_{\text{eff}}$  are determined by

$$R_V = -24\frac{b}{a}, \quad V_{\text{eff}} = \frac{4C_4}{a}. \quad (15)$$

The constant  $C_4$  in equation (10) is  $\pi^2/2$ . In flat space we would have  $V_{\text{eff}} = V_4$ , giving

$$a = \frac{4C_4}{V_4} = \frac{48\sqrt{5}\pi^2}{125} \approx 8.47, \quad (16)$$

where we used  $V_4 = 25\sqrt{5}/24$  for  $\ell = \sqrt{10}$ . Such a space cannot be formed from equilateral simplices because we cannot fit an integer number of simplices in an angle of  $2\pi$  around a triangle. We expect therefore  $V_{\text{eff}}$  to be different from  $V_4$ .

Figure 2 shows  $N'(r)$  for 16000 simplices. Three different values of  $\kappa_2$  are shown, 0.8 (in the crumpled phase), 1.22 (close to the transition) and 1.5 (in

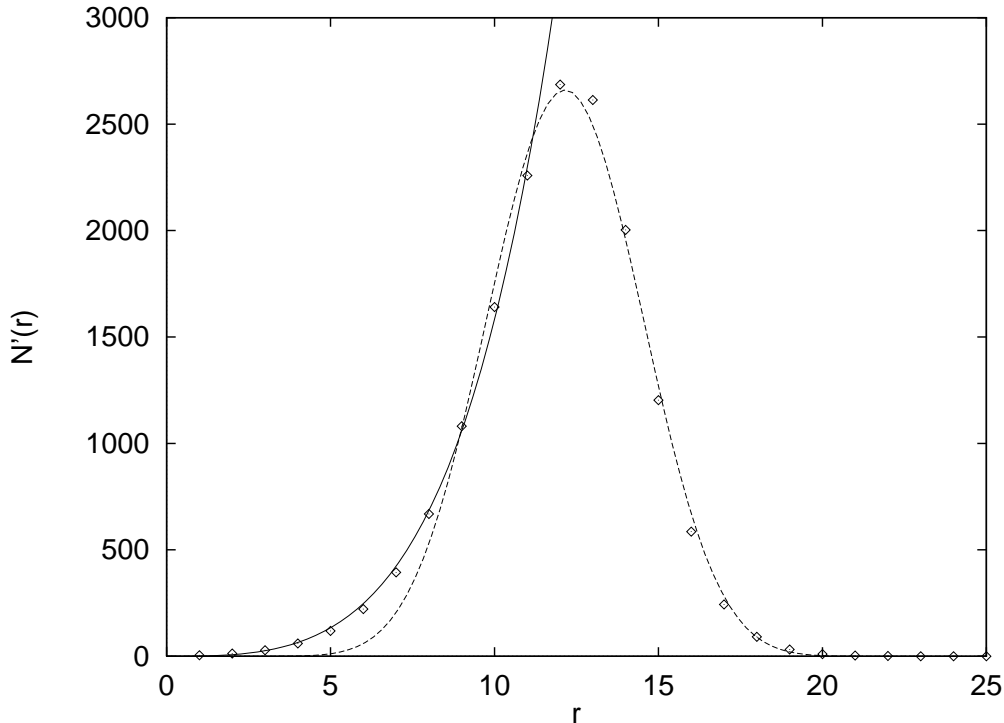


Figure 3: Effective curvature fit and global dimension fit in the crumpled phase at  $\kappa_2 = 0.80$ .

the elongated phase). These curve can also be interpreted as the probability distribution of the geodesic length between two simplices. Such distributions were previously presented in refs. [3, 5].

We determined  $N'(r)$  by first averaging this value per configuration successively using each simplex as the origin. We then used a jackknife method, leaving out one configuration each time, to determine the error in  $R_V$ .

Our results in this paper are based on  $N = 8000$  and  $16000$  simplices. Configurations were recorded every  $10000$  sweeps, where a sweep is defined as  $N$  accepted moves. The time before the first configuration was recorded was also  $10000$  sweeps. We estimated the autocorrelation time in the average distance between two simplices to be roughly  $2000$  sweeps for  $N = 16000$  and  $\kappa_2 = 1.22$ . For other values of  $\kappa_2$  the autocorrelation time was lower. The number of configurations at the values of  $\kappa_2$  used are shown in table 1.

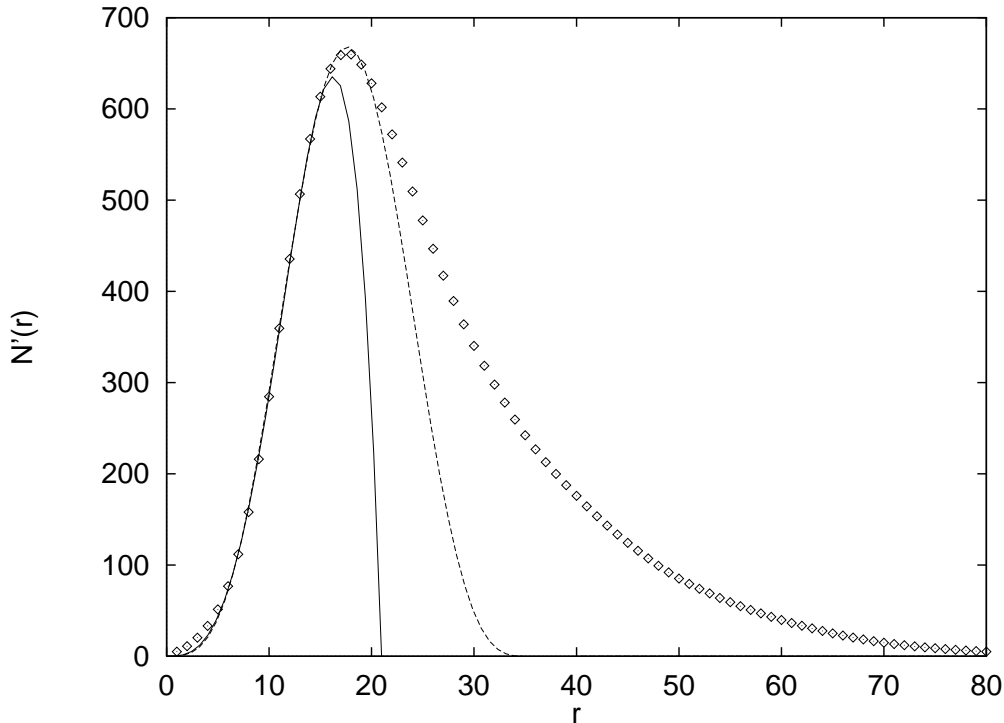


Figure 4: Effective curvature fit and global dimension fit near the transition,  $\kappa_2 = 1.22$ .

Figures 3–5 show effective curvature fits (continuous lines) in the crumpled phase ( $\kappa_2 = 0.80$ ), near the transition ( $\kappa_2 = 1.22$ ) and in the elongated phase ( $\kappa_2 = 1.50$ ), together with global dimension fits (see the next section) at longer distances, for  $N = 16000$ . The curves are extended beyond the fitted data range,  $r = 1$ – $11$ , to indicate their region of validity. A least squares fit was used, which suppresses the lattice artefact region where  $N'(r)$  is small because it is sensitive to absolute errors rather than relative errors.

For  $\kappa_2 \lesssim \kappa_2^c$  the fits were good even beyond the range of  $r$  used to determine the fit (except obviously when this range already included all the points up to the maximum of  $N'(r)$ ). This can be seen in figure 4, where the fit is good up to  $r = 15$ . The fit with  $ar^3 + br^5$  does not appear sensible anymore for  $\kappa_2$  values somewhat larger than the critical value  $\kappa_2^c$ , because then  $N'(r)$  goes roughly linear with  $r$  down to small distances. This can be seen quite

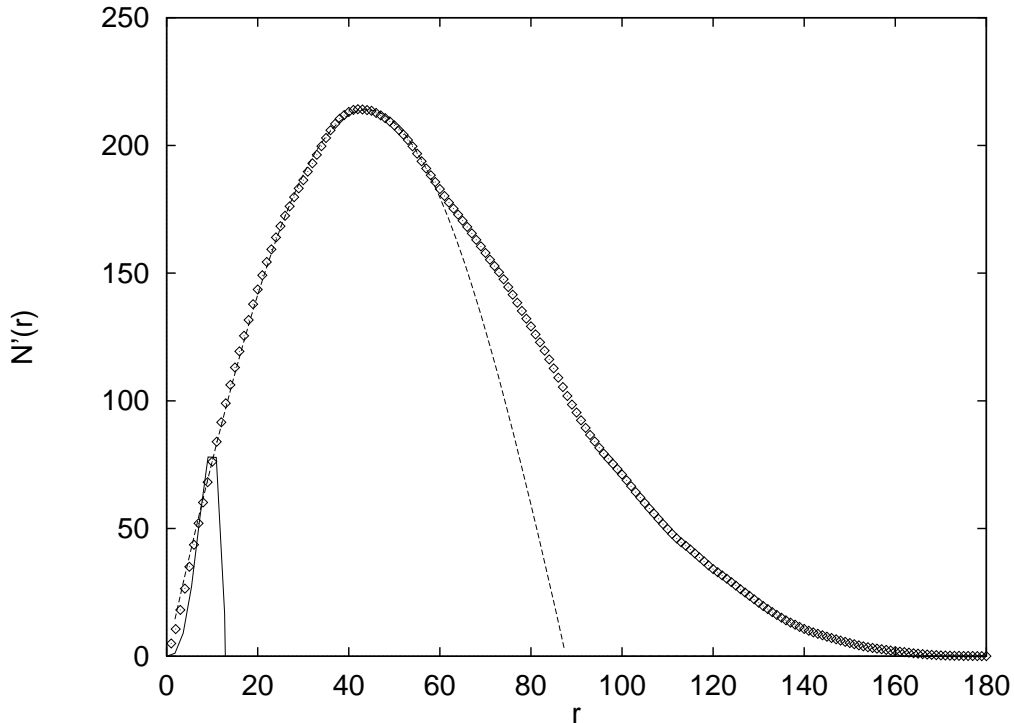


Figure 5: Effective curvature fit and global dimension fit in the elongated phase at  $\kappa_2 = 1.50$  (the effective curvature fit is not appropriate here).

clearly in figure 5 (so the  $R_V$  fit in this figure should be ignored).

Figure 6 shows the resulting effective curvature  $R_V$  as a function of  $\kappa_2$  for 8000 and 16000 simplices. For  $N = 8000$  the fitting range was  $r = 1-9$ . We see that  $R_V$  starts negative and then rises with  $\kappa_2$ , going through zero. In contrast, the Regge curvature at the triangles  $\langle \bar{R} \rangle$  is positive for all  $\kappa_2$  values in the figure.

The value of  $a$  in (15) varied from about 0.9 at  $\kappa_2 = 0.8$  to 0.4 near the transition. These numbers are much smaller than the flat value of 8.47 in equation (16), indicating an effective volume per simplex  $V_{\text{eff}} \approx 20 - 50$ , much larger than  $V_4 \approx 2.3$ . This is at least partly due to the way we measure distances. The distances are measured using paths which can only go along the dual lattice and will therefore be larger than the shortest paths through the simplicial complex.

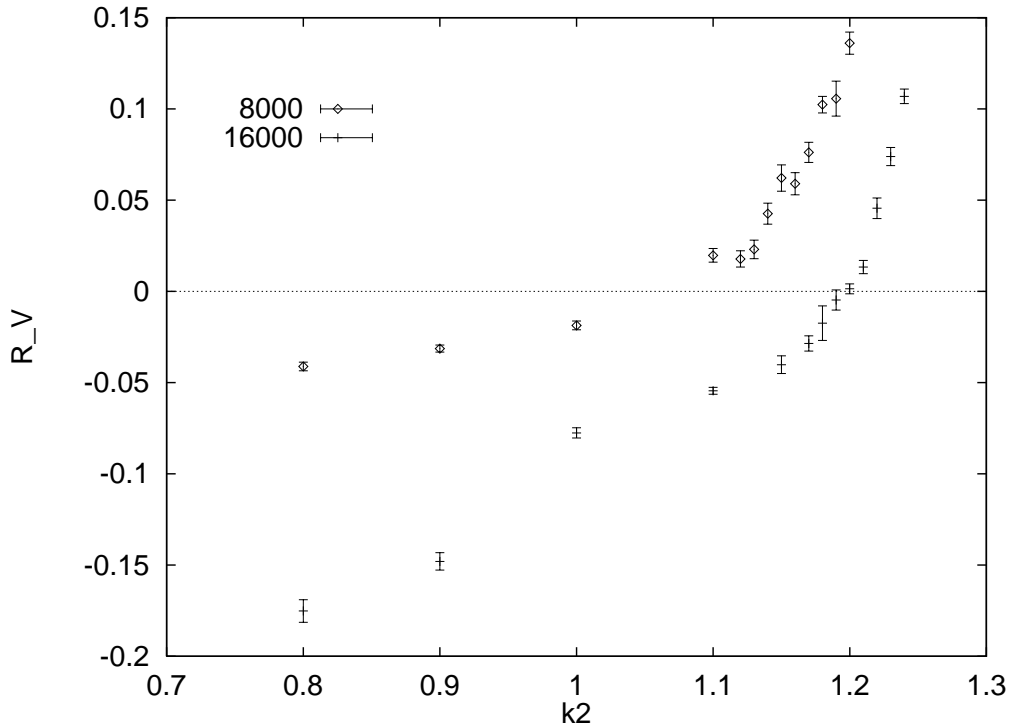


Figure 6: The effective curvature  $R_V$  as a function of  $\kappa_2$  for 8000 and 16000 simplices.

There is a strong systematic dependence of  $R_V$  on the range of  $r$  used in the fit. For example, for the  $N = 16000$  data in figure 6 we used a least squares fit in the range  $r = 1-11$ . If the range is changed to  $r = 1-9$  the data for  $R_V$  have to be multiplied with a factor of about 1.5. We can enhance this effect by reducing the fitting range to only two  $r$  values and thereby obtain a ‘running curvature’  $R_{\text{eff}}(r)$  at distance  $r$ . We write  $N'(r) = a(r)r^3 + b(r)r^5$ ,  $N'(r+1) = a(r)(r+1)^3 + b(r)(r+1)^5$  and define  $R_{\text{eff}}(r + \frac{1}{2}) = -24b(r)/a(r)$ , which gives

$$R_{\text{eff}}(r + \frac{1}{2}) = 24 \frac{(r+1)^3 - r^3 N'(r+1)/N'(r)}{(r+1)^5 - r^5 N'(r+1)/N'(r)}. \quad (17)$$

Figure 7 shows the behavior of  $R_{\text{eff}}(r)$  for various  $\kappa_2$ . It drops rapidly from large values  $\approx 4.5$  (which is near  $\langle \bar{R} \rangle \approx 5.5$ ) at  $r = 0$  to small values at

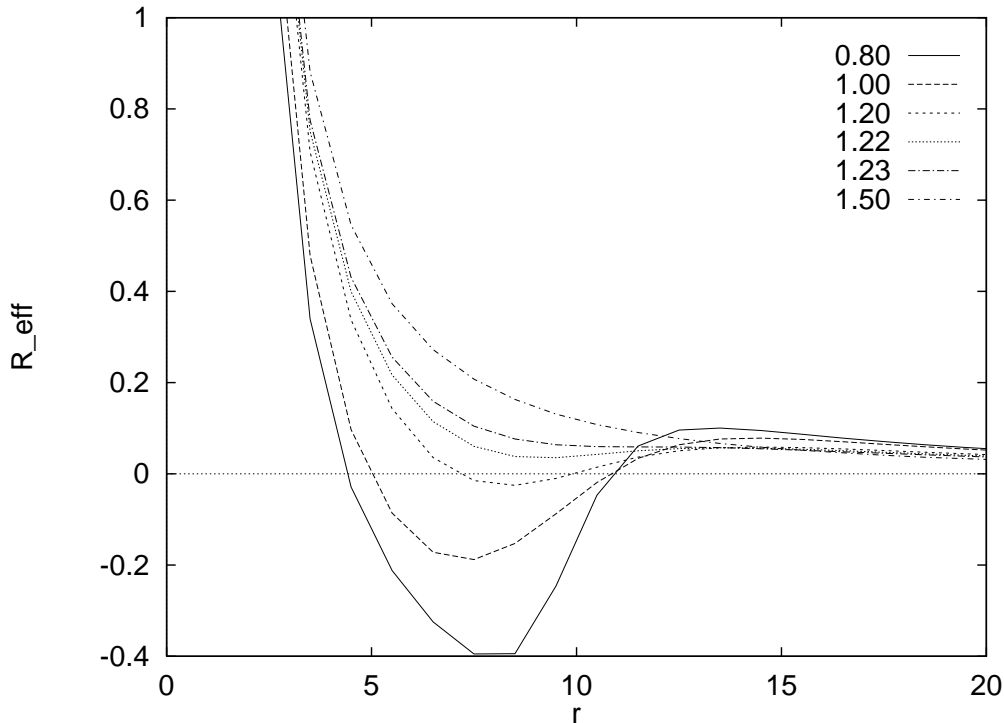


Figure 7: The effective curvature  $R_{\text{eff}}(r)$  for various  $\kappa_2$  and 16000 simplices.

$r \approx 8$ . For  $\kappa_2 \lesssim \kappa_2^c$  the curves have a minimum and around this minimum the values of  $R_{\text{eff}}$  average approximately to the  $R_V$ 's displayed earlier.

The idea of  $R_{\text{eff}}(r)$  and  $R_V$  is to measure curvature from the correlation function  $N'(r)$  by comparing it with the classical volume-distance relation for distances  $r$  going to zero, as long as there is reasonable indication for classical behavior at these distances. Clearly, we cannot let  $r$  go to zero all the way because of the huge increase of  $R_{\text{eff}}$ . This seems to indicate a ‘planckian regime’ where classical behavior breaks down.

### 3 Dimension

One of the interesting observables in the model is the dimension at large scales. A common way to define a fractal dimension is by studying the behaviour of the volume within a distance  $r$  and identifying the dimension  $d$

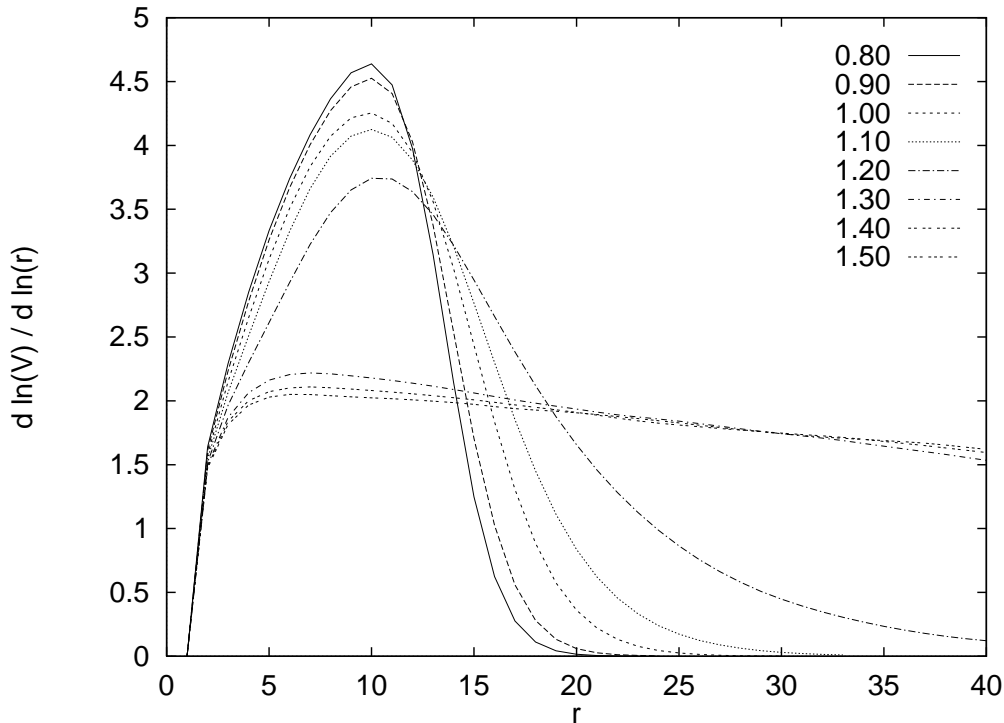


Figure 8:  $\ln[(N(r)/N(r-1))]/\ln[r/(r-1)] \longleftrightarrow d \ln V/d \ln r$  as a function of  $r$  for some values of  $\kappa_2$ .

if the volume behaves like

$$V(r) = \text{const.} \times r^d. \quad (18)$$

Such a measurement has been done in [1, 2], using the geodesic distance and a distance defined in terms of the massive scalar propagator [14]. Arguments against the necessity of such use of the massive propagator were raised in ref. [16]. Although we feel that the issue is not yet settled, we shall use here the geodesic distance as in the previous section.

If the volume does go like a power of  $r$ , the quantity

$$d = \frac{d \ln V}{d \ln r} \longleftrightarrow \frac{\ln N(r) - \ln N(r-1)}{\ln(r) - \ln(r-1)}, \quad (19)$$

would be a constant. Figure 8 shows this quantity for some values of  $\kappa_2$  for a system with 16000 simplices. We see a sharp rise at distances  $r =$

1, 2 independent of  $\kappa_2$  which is presumably a lattice artefact. The curves then continue to rise until a maximum where we may read off an effective dimension, which is clearly different in the crumpled phase ( $\kappa_2 = 0.80\text{--}1.20$ ) and in the elongated phase ( $\kappa_2 = 1.30\text{--}1.50$ ). Instead of a local maximum one would of course like a plateau of values where  $d \ln V/d \ln r$  is constant and may be identified with the dimension  $d$ . Only for  $\kappa_2$  beyond the transition a range of  $r$  exists where  $d \ln V/d \ln r$  looks like a plateau. In this range,  $d \approx 2$ .

Similar studies have been carried out in 2D dynamical triangulation where it was found that plateaus only appear to develop for very large numbers of triangles [15]. Our 4D systems are presumably much too small for  $d \ln V/d \ln r$  to shed light on a fractal dimension at large scales, if it exists. However, we feel that the approximate plateau in the elongated phase with  $d = 2$  should be taken seriously.

As we are studying a system with the topology of the sphere  $S^4$ , it seems reasonable to look whether it behaves like a  $d$ -dimensional sphere  $S^d$ . For such a hypersphere with radius  $r_0$ , the volume behaves like

$$V'(r) = dC_d r_0^{d-1} \left(\sin \frac{r}{r_0}\right)^{d-1}. \quad (20)$$

This prompts us to explore (20) as a definition of the dimension  $d$ , we shall call it the global dimension. For small  $r/r_0$  this reduces to (18). On the other hand for  $d = n$  the form (20) is compatible with the effective curvature form (12), with

$$R_V = \frac{n(n-1)}{r_0^2}. \quad (21)$$

To determine the dimension  $d$  we fit the data for  $N'(r)$  to a function of the form (20),

$$N'(r) = c \left(\sin \frac{r}{r_0}\right)^{d-1}. \quad (22)$$

The free parameters are  $r_0$ ,  $d$  and the multiplicative constant  $c$ . It is a priori not clear which distances we need to use to make the fit. At distances well below the maximum of  $N'(r)$  (cf. figure 2) the effective curvature fit appears to give a reasonable description of the data, but it will be interesting to try (20) also for these distances. Small distances are of course affected by the discretization. This is most pronounced at low  $\kappa_2$  where the range of  $r$ -values is relatively small. On the other hand, for small  $\kappa_2$  the fits turn out

to be good up to the largest distances, indicating a close resemblance to a hypersphere, while at larger  $\kappa_2$  the values of  $N'(r)$  are asymmetric around the peak (cf. fig. 2) and fits turn out to be good only up to values of  $r$  not much larger than this peak. The system behaves like a hypersphere up to the distance where  $N'(r)$  has its maximum, which would correspond to halfway the maximum distance for a real hypersphere. Above that distance it starts to deviate, except for small  $\kappa_2$  where  $N'(r)$  is more symmetric around the peak and the likeness remains.

For  $\kappa_2 = 0.8$  (figure 3) the global dimension fit (22) was performed to the data at  $r = 7-21$ , for  $\kappa_2 = 1.22$  (figure 4) to  $r = 4-20$  and for  $\kappa_2 = 1.50$  (figure 5) to  $r = 3-60$ .

The two descriptions, effective curvature at lower distances and effective dimension at intermediate and larger distances, appear compatible. Notice that at  $\kappa_2 = 0.8$  in the crumpled phase the local effective curvature  $R_V$  is negative while the global structure resembles closely a (positive curvature) sphere with radius  $r_0 = 7.6$  ( $r_0 = 2r_m/\pi$ , with  $r_m$  the value where  $N'(r)$  is maximal). At  $\kappa_2 = 1.22$  near the transition the effective curvature and effective dimension descriptions appear to coincide. At  $\kappa_2 = 1.50$ , deep in the elongated phase, the effective curvature fit does not make sense anymore, its  $r$ -region of validity has apparently shrunk to order 1 or less. The effective dimension fit on the other hand is still good in this phase and the power behavior (18) with  $d \approx 2$  is extended by (22) to intermediate distances including the maximum of  $N'(r)$ .

Figure 9 shows the global dimension as a function of  $\kappa_2$  for the total volumes of 8000 and 16000 simplices. For small values of  $\kappa_2$  it is high and increases with larger volumes. For values of  $\kappa_2$  beyond the transition it quickly goes to two, confirming the statement made earlier that in this region  $N'(r)$  is approximately linear with  $r$  down to small  $r$ .

A most interesting value of the dimension is the one at the phase transition. To determine the value of  $\kappa_2^c$  where the transition takes place we look at the curvature susceptibility of the system, figure 1. For 8000 simplices the peak in the susceptibility is between  $\kappa_2$  equals 1.17 and 1.18 where the dimensions we measured are 4.2(1) and 3.8(1). For 16000 simplices the peak is between 1.22 and 1.23 where the dimensions are 4.2(1) and 3.6(1). Therefore the dimension at the transition is consistent with 4. As can be seen from these numbers the largest uncertainty in the dimension is due to the uncertainty in  $\kappa_2^c$ . The effective dimensions have some uncertainty due

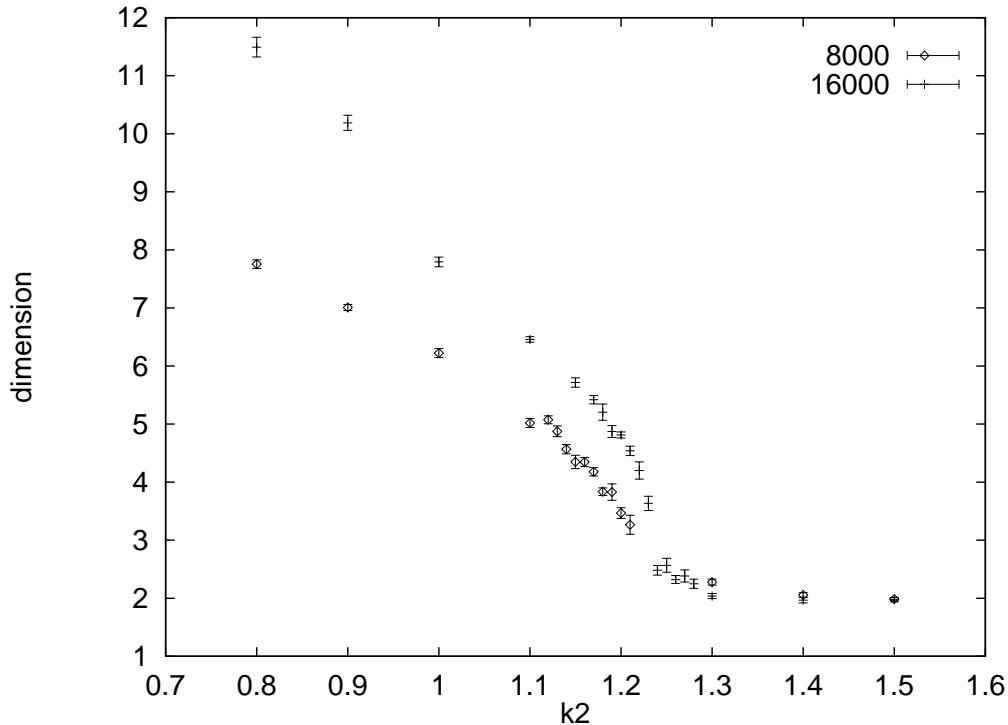


Figure 9: The global dimension as a function of  $\kappa_2$  for 8000 and 16000 simplices.

to the ambiguity of the range of  $r$  used for the fit. Near the transition this generates an extra error of approximately 0.1.

## 4 Scaling

To get a glimpse of continuum behavior it is essential to find scaling behavior in the system. We found a behavior like a  $d$  dimensional hypersphere for  $r$  values up to the value  $r_m$  where  $N'(r)$  is maximal. This suggests scaling in the form

$$N'(r) = r_m^{d-1} f\left(\frac{r}{r_m}, d\right), \quad (23)$$

i.e.  $N'(r)$  depends on  $\kappa_2$  and  $N$  through  $d = d(\kappa_2, N)$  and  $r_m = r_m(\kappa_2, N)$ . The occurrence of  $d$  in this formula is unattractive, however, since it is ob-

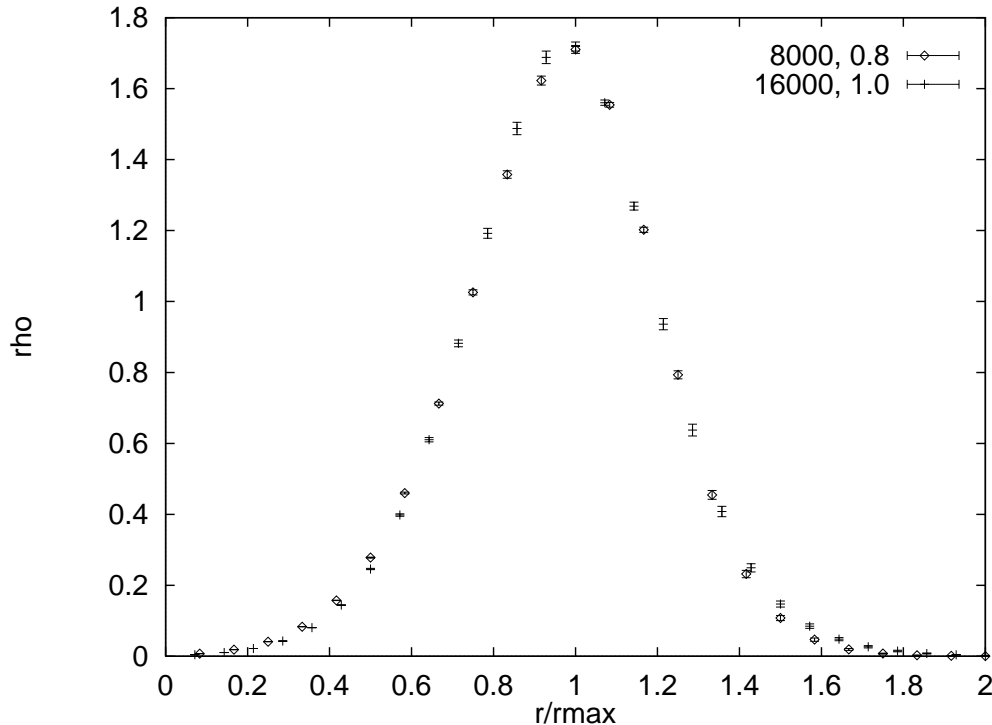


Figure 10: The scaling function  $\rho$  for  $\kappa_2 = 0.8$  at  $N = 8000$  and  $\kappa_2 = 1.0$  at  $N = 16000$ .

tained by comparing  $N'(r)$  to  $\sin^{d-1}(r/r_0)$  at intermediate scales, which is a somewhat imprecise concept. We would like a model independent test of scaling.

Consider the probability for two simplices to have a geodesic distance  $r$ ,

$$p(r) = \frac{N'(r)}{N}, \quad 1 = \sum_{r=1}^{\infty} p(r) \approx \int dr p(r), \quad (24)$$

which depends parametrically on  $\kappa_2$  and  $N$ . It seems natural to assume scaling for this function in the form

$$p(r) = \frac{1}{r_m} \rho\left(\frac{r}{r_m}, \tau\right), \quad \int dx \rho(x, \tau) = 1, \quad (25)$$

where  $\tau$  is a parameter playing the role of  $d$  in (23) which labels the different functions  $\rho$  obtained this way. For instance,  $\tau$  could be the value  $\rho_m = \rho(1, \tau)$

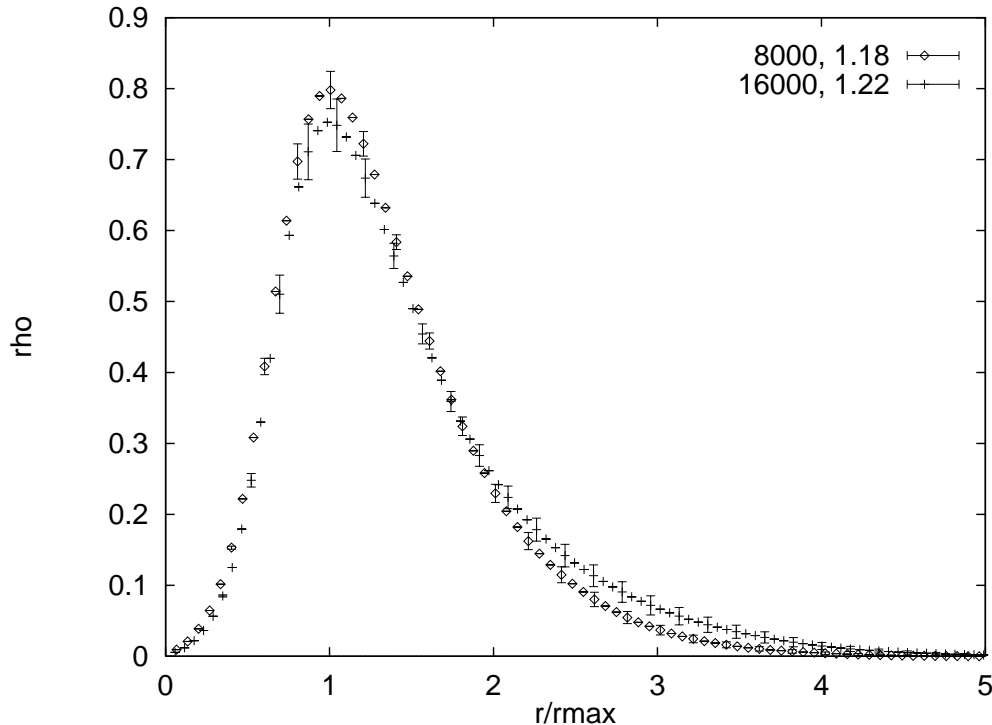


Figure 11: The scaling function  $\rho$  for  $\kappa_2 = 1.18$  at  $N = 8000$  and  $\kappa_2 = 1.22$  at  $N = 16000$ .

at the maximum of  $\rho$ . This may give give problems if  $\rho_m$  does not change appreciably with  $\kappa_2$  (similar to  $d$  in the elongated phase). Other possibilities are  $\tau = \bar{r}p(r_m)$  or  $\tau = \bar{r}^k/\bar{r}^k$  for some  $k$  with  $\bar{r}^k = \sum_r p(r)r^k$ . In practice we may also simply take  $\tau = \kappa_2 - \kappa_2^c(N)$  at some standard choice of  $N$  and compare the probability functions with the  $p(r)$  at this  $N$ .

Matched pairs of  $\rho(x, \tau)$  for  $N = 8000$  and  $16000$  are shown in figures 10–12, respectively far in the crumpled phase, near the transition and in the elongated phase. For clarity we have left out part of the errors. Scaling appears to hold even for  $\kappa_2$  values we considered far away from the transition.

The values of  $\kappa_2(N)$  of the matched pairs in figs. 10–12 are increasing with  $N$  in the crumpled phase and decreasing with  $N$  in the elongated phase. This suggests convergence from both sides to  $\kappa_2^c(N)$  as  $N$  increases. For current system sizes  $\kappa_2^c(N)$  is still very much dependent on  $N$ , a power extrapolation estimate [8] gives  $\kappa_2^c(\infty) \approx 1.45$ .

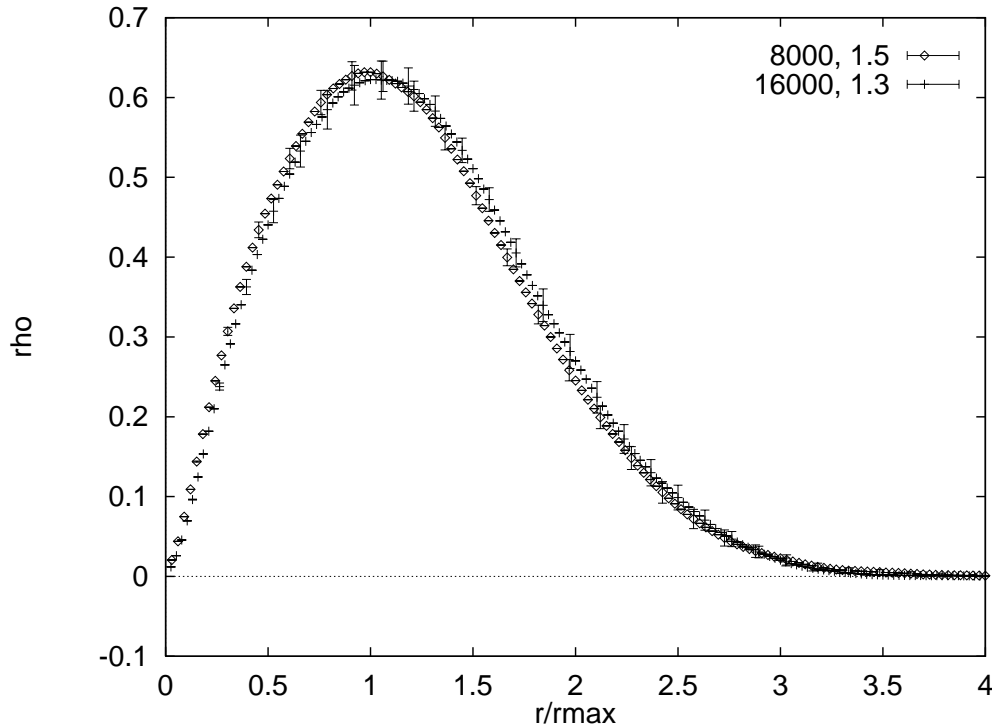


Figure 12: The scaling function  $\rho$  for  $\kappa_2 = 1.5$  at  $N = 8000$  and  $\kappa_2 = 1.3$  at  $N = 16000$ .

We can use the matched pairs of  $\rho$  to define a scaling dimension  $d_s$  by

$$N = \alpha r_m^{d_s}, \quad (26)$$

where  $\alpha$  and  $d_s$  depend only on  $\tau$ . Using non-lattice units, replacing the integer  $r_m$  by  $r_m/(\ell/\sqrt{10})$  where  $r_m$  is now momentarily dimensionful, we can interpret (26) as

$$N \propto \left(\frac{r_m}{\ell}\right)^{d_s}, \quad (27)$$

which shows that the scaling dimension characterizes the dimensionality of the system at small scales  $\ell \rightarrow 0$  with  $r_m$  fixed. Returning to lattice units, taking for  $r_m$  the integer value of  $r$  where  $N'(r)$  is maximal and using an assumed error of 0.5, these scaling dimensions would be 4.5(3), 3.8(2) and 4.0(1) respectively for figures 10, 11 and 12. The largest errors in these figures

probably arises due to the uncertainty in the values of  $\kappa_2$  we need to take to get matching curves, i.e. to get the same value of  $\tau$ . As we do not have data for a continuous range of  $\kappa_2$  values, we have to make do with what seems to match best from the values we do have. Nevertheless, the values of  $d_s$  far away from the transition are strikingly close to 4 when compared to the values of the global dimension  $d$ , which are 7.8 and 2.0 for figures 10 and 12.

The scaling form (23) is in general incompatible with (25), except for  $d_s = d$ . The evidence for  $d_s = 4$  points instead to a scaling behavior of the form

$$N'(r) = r_m^3 f\left(\frac{r}{r_m}, \tau\right), \quad (28)$$

with  $f(x, \tau) = \alpha(\tau)\rho(x, \tau)$ . This further suggests scaling of the volume  $V'(r)$  at distance  $r$  with an effective volume  $V_{\text{eff}}$  per simplex (cf. (13)) depending only on  $\tau$ .

A precise definition of the scaling form  $\rho(x, \tau)$  may be given by

$$\rho(x, \tau) = r_m p(r_m x), \quad \kappa_2 = \kappa_2(N) \text{ such that } r_m p(r_m) = \tau, \quad N \rightarrow \infty, \quad (29)$$

where we used  $\tau = \rho_m$  for illustration. Intuitively one would expect the convergence to the scaling limit (29) to be non-uniform, with the large  $x$  region converging first, and there may be physical aspects to such nonuniformity.

The scaling analogue of running curvature (17) is given by

$$\tilde{R}(x) \equiv r_m^2 R_{\text{eff}}(xr_m) = \frac{24}{x^2} \frac{3 - d \ln \rho / d \ln x}{5 - d \ln \rho / d \ln x}. \quad (30)$$

Fig. 13 shows this function for the matched pair of fig. 11 in the transition region. We have also included the curve for  $\kappa_2 = 1.23$  at  $N = 16000$ . The curves do not match in the region around  $x = 0.5$  and  $R_{\text{eff}}$  is apparently a sensitive quantity for scaling tests. Still, fig. 13 suggests reasonable matching for a value of  $\kappa_2(16000)$  somewhere between 1.22 and 1.23 and even the steep rise as far as shown appears to be scaling approximately, with  $\tilde{R}(16000)$  somewhat below  $\tilde{R}(8000)$ . We find similar scaling behavior for the matched pair in the elongated phase. The number of our  $\kappa_2$  values in the crumpled phase is too limited to be able to draw a conclusion there.

The steep rise appears to move to the left for increasing  $N$  (a scaling violation). A most interesting question is whether the onset of the rise (e.g. the  $x$  value where  $\tilde{R} = 50$ ) continues to move towards  $x = 0$  as  $N \rightarrow \infty$ . Such

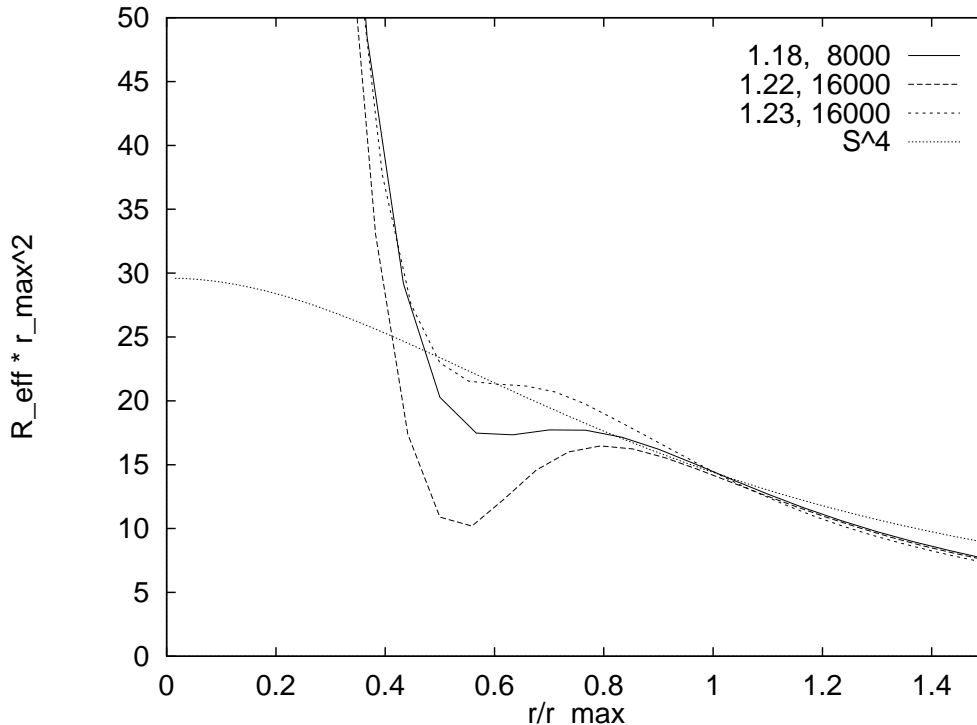


Figure 13: Scaling form  $r_m^2 R_{\text{eff}}(xr_m)$  versus  $r/r_m$  near the transition, for  $N = 8000$ ,  $\kappa_2 = 1.18$  (middle) and  $N = 16000$ ,  $\kappa_2 = 1.22, 1.23$  (lower and upper). The hypothetical limiting form corresponding to  $S^4$  is also shown.

behavior is needed for a classical region to open up from  $x$  around 1 towards the origin  $x = 0$ . In other words, the ‘planckian regime’ would have to shrink in units of the size  $r_m$  of the ‘universe’. Then  $r_m^2 R_V$  could be defined as a limiting value of  $\tilde{R}$ ,  $x \rightarrow 0$ .

Since we are looking for classical behavior in the transition region it is instructive to compare with the classical form of  $\tilde{R}$  corresponding to the sphere  $S^4$ , for which  $\rho = \rho_m \sin^3 \theta$ ,  $\theta = \pi x/2$ ,

$$\tilde{R} = \frac{18\pi^2}{\theta^2} \frac{\tan \theta - \theta}{5 \tan \theta - 3\theta} = 3\pi^2 \left(1 - \frac{13\pi^2}{120} x^2 + \dots\right). \quad (31)$$

This function is also shown in fig. 13. Our current data are evidently still far from the hypothetical classical limiting form (31).

## 5 Summary

The average number of simplices  $N'(r)$  at geodesic distance  $r$  gives us some basic information on the ensemble of euclidean spacetimes described by the partition function (1). The function  $N'(r)$  is maximal at  $r = r_m$  and  $r_m N'(r)/N$  shows scaling when plotted as a function of  $r/r_m$ . We explored a classical definition of curvature in the small to intermediate distance regime based on spacetime dimension four, the effective curvature  $R_V$ . We also explored a description at global distances by comparing  $N'(r)$  with a sphere of effective dimension  $d$ . Judged by eye, the effective curvature fits and effective dimension fits give a reasonable description of  $N'(r)$  in an appropriate distance regime (figs. 3–5). The resulting  $R_V$  depends strongly on the fitting range, which led us to an explicitly distance dependent quantity, the ‘running’ curvature  $R_{\text{eff}}(r)$ . This dropped rapidly from lattice values of order of the Regge curvature at  $r = 0$  to scaling values of order of the  $R_V$  found in the effective curvature fits at intermediate distances. A preliminary analysis of scaling behavior then suggested the possibility of a classical regime with a precise definition of  $r_m^2 R_V$  in the limit of large  $N$ . We shall now summarize the results further, keeping in mind the ambiguity in  $R_V$  as derived from the fits to  $N'(r)$ .

For small  $\kappa_2$  the effective curvature is negative. Furthermore the system resembles a  $d$ -sphere with very large dimension  $d$  which increases with the volume. This suggests that no matter how large the volumes we use, there will never be a region of  $r$  where the power law  $V(r) \propto r^d$  gives good fits over large ranges of  $r$ . In other words, the curves for  $d \ln V/d \ln r$  in figure 8 will never have a plateau. This behavior is consistent with that of a space with constant negative curvature, where the volume rises exponentially with the geodesic distance for distances larger than the curvature radius and if we look at large enough scales the intrinsic fractal dimension equals infinity. The resulting euclidean spacetime cannot be completely described as a space with constant negative curvature as such a space with topology  $S^4$  does not exist, and finite size effects take over at still larger distances.

At the transition the spacetime resembles a 4-dimensional sphere with small positive effective curvature, up to intermediate distances.

For large  $\kappa_2$  the system has dimension 2. In this region it appears to behave like a branched polymer, which has an intrinsic fractal dimension of 2 [14]. Moving away from the transition, the curvature changes much

more rapidly than in the small  $\kappa_2$  phase and the effective curvature radius  $r_V$  soon becomes of the order of the lattice distance. A priori, two outcomes seem plausible. In the first, the system collapses and  $r_V$  becomes of order 1 in lattice units, reflecting the unboundedness of the continuum action from below. In the second, the spacetime remains 4-dimensional and  $r_V$  can still be tuned to large values in lattice units, but very small compared to the global size  $r_m$ , for a sufficiently large system. So far the second outcome seems to be favored, for two reasons. Firstly, the function  $N'(r)$  looks convex for  $r \leq 6$  slightly above the transition, e.g. for  $\kappa_2 = 1.24$  at 16000 simplices. In other words, the linear behavior as seen in figure 5 does not set in immediately above the transition. Secondly, the system shows scaling and the scaling dimension  $d_s$  as defined in (26) is approximately 4 even far into the elongated phase, indicating 4-dimensional behavior at small scales.

High and low dimensions in the crumpled and elongated phases with the value four at the transition were reported earlier in ref. [2]. This dimension was apparently interpreted as a small scale dimension, whereas instead we find a small scale dimension of four in all phases. Similar results are also found in the Regge calculus approach to quantum gravity [17, 18], where one also finds two phases, a strong (bare Newton) coupling phase with negative curvature and fractal dimension four, and (using an  $R^2$  term in the action for stabilization) a weak coupling phase with fractal dimension around two.

## 6 Discussion

The evidence for scaling indicates continuum behavior. This brings up a number of issues which need to be addressed in a physical interpretation of the model.

One guideline in this work is the question whether there is a regime of distances where  $V'(r) = V_{\text{eff}}N'(r)$  behaves classically for suitable bare Newton constant  $G_0$ . The connection with classical spacetime can be strengthened by identifying the geodesic distance  $r$  with a cosmic time  $t$  and  $V'(r)^{1/3}$  with the scale factor  $a(t)$  in a euclidean Robertson-Walker metric. The classical action for  $a(r)$  is given by

$$S = -\frac{\pi}{8G} \int dr \left[ a \left( \frac{da}{dr} \right)^2 + a \right] + \lambda \left( 2\pi^2 \int dr a^3 - V \right), \quad (32)$$

where  $\lambda$  is a Lagrange multiplier enforcing a total spacetime volume  $V$ . It plays the role of a cosmological constant which is just right for getting volume  $V$ . For positive  $G\lambda$  the solution of the equations of motion following from (32) is  $a = r_0 \sin r/r_0$ , which represents  $S^4$  with  $R = 12/r_0^2 = 192\pi G\lambda$ . For negative  $G\lambda$  the solution is  $a = r_0 \sinh r/r_0$  which represents a space of constant negative curvature  $R = -12/r_0^2 = 192\pi G\lambda$ , cut off at a maximal radius to get total volume  $V$ .

The form (32) serves as a crude effective action for the system for intermediate distances around the maximum in  $V'(r)$  at  $r_m$ , and couplings  $\kappa_2 \propto G_0^{-1}$  in the transition region. At larger distances the fluctuations of the spacetimes grow, causing large baby universes and branching, and averaging over these may be the reason for the asymmetric shape of  $V'(r)$ . Because of this the Robertson-Walker metric cannot give a good description at these distances.

Intuitively one expects also strong deviations of classical behavior at distances of order of the Planck length  $\sqrt{G}$ , assuming that a Planck length exists in the model. A proposal for measuring it was put forward in [19]. The steep rise in the running curvature  $R_{\text{eff}}(r)$  at smaller  $r$  indeed suggests such a planckian regime. It extends to rather large  $r$  but it appears to shrink compared to  $r_m$  as the lattice distance decreases, i.e.  $N$  increases for a given scaling curve labelled by  $\tau$ . This suggests that the Planck length goes to zero with the lattice spacing,  $G/r_m^2 \rightarrow 0$  as  $N \rightarrow \infty$  at fixed  $\tau$ . This does not necessarily mean that the Planck length is of order of the lattice spacing, although this is of course quite possible. However, the theory may also scale at planckian distances and belong to a universality class. It might then be ‘trivial’.

At this point it is instructive to recall other notorious models with a dimensionful coupling as in Einstein gravity, the 4D nonlinear sigma models. The lattice models have been well studied, in particular the  $O(4)$  model for low energy pion physics (see for example [20]). It has one free parameter  $\kappa = \ell^2 f_0^2$  which corresponds to the renormalized dimensionful coupling  $f^2$ ;  $f$  is the pion decay constant or the electroweak scale in the application to the Standard Model. With this one bare parameter it is possible to tune *two* quantities,  $f/m$  and  $\ell f$ , where  $m$  is the mass of the sigma particle or the Higgs particle. This trick is possible because the precise value of  $\ell$  is

unimportant, as long as it is sufficiently small<sup>†</sup>. However, in the continuum limit  $\ell f \rightarrow 0$  triviality takes its toll:  $m/f \rightarrow 0$  and the model becomes noninteracting. The analogy  $f^2 \leftrightarrow 1/G$ ,  $m \leftrightarrow r_m^{-1}$  suggests that we may be lucky and there is a scaling region in  $\kappa_2$ - $N$  space, for a given scaling curve (given  $\tau$ ), where the theory has universal properties and where we can tune  $G/r_m^2$  to a whole range of desired values. Taking the scaling *limit* however might lead to a trivial theory with  $G/r_m^2 = 0$ . In case this scenario fails it is of course possible to introduce more parameters, e.g. as in  $R^2$  gravity, to get more freedom in the value of  $G/r_m^2$ . This then raises the question of universality at the Planck scale.

We really would like to replace  $r_m^2$  by  $R_V$  in the reasoning in the previous paragraph, since we view  $R_V$  as the local classical curvature, provided that a classical regime indeed develops as  $N \rightarrow \infty$ .

Next we discuss the nature of the elongated phase. Even deep in this phase we found evidence for scaling. Furthermore, for given scaling curve, increasing  $N$  means decreasing  $\kappa_2$ . Hence, increasing  $N$  at fixed  $\kappa_2$  brings the system deeper in the elongated phase. This leads to the conclusion that there is nothing wrong with the elongated phase. It describes very large spacetimes which are two dimensional on the scale of  $r_m$  but not necessarily at much smaller scales. It could be effectively classical at scales much larger than the Planck length but much smaller than  $r_m$ .

This reasoning further suggests that  $N$  and  $\kappa_2$  primarily serve to specify the ‘shape’ of the spacetime. The tuning  $\kappa_2 \approx \kappa_2^c$  is apparently not needed for obtaining criticality but for obtaining a type of spacetime. The peak in the susceptibility of the Regge curvature could be very much a reflection of shape dependence. Most importantly, this suggests that the physical properties associated with general coordinate invariance will be recovered automatically in 4D dynamical triangulation, as in 2D with fixed topology<sup>‡</sup>.

---

<sup>†</sup>It is good to keep the numbers in perspective: for example in the Standard Model  $f = 250$  GeV and for a Higgs mass  $m = 100$  GeV or less,  $\ell$  is 15 orders of magnitude smaller than the Planck length, or even much smaller.

<sup>‡</sup>A field theory analogue is  $Z_n$  lattice gauge theory, which for  $n \geq 5$  has been found to possess a Coulomb phase, a whole region in bare parameter space with massless photons; see for example ref. [21].

## Acknowledgements

This work is supported in part by the Stichting voor Fundamenteel Onderzoek der Materie (FOM). The numerical simulations were partially carried out on the IBM SP1 at SARA.

## References

- [1] M.E. Agishtein and A.A. Migdal, Mod. Phys. Lett. A7 (1992) 1039.
- [2] M.E. Agishtein and A.A. Migdal, Nucl. Phys. B385 (1992) 395.
- [3] J. Ambjørn and J. Jurkiewicz, Phys. Lett. B278 (1992) 42.
- [4] D. Weingarten, Nucl. Phys. B210 (1982) 229.
- [5] J. Ambjørn, J. Jurkiewicz and C.F. Kristjansen, Nucl. Phys. B393 (1993) 601.
- [6] S. Varsted, Nucl. Phys. B412 (1994) 406.
- [7] B. Brüggmann, Phys. Rev. D47 (1993) 3330.
- [8] S. Catterall, J. Kogut and R. Renken, Phys. Lett. B28B (1994) 277.
- [9] J. Ambjørn, S. Jain, J. Jurkiewicz and C.F. Kristjansen, Phys. Lett. B305 (1993) 208.
- [10] S. Catterall, J. Kogut and R. Renken, Phys. Rev. Lett. 72 (1994) 4062.
- [11] J. Ambjørn and J. Jurkiewicz *On the exponential bound in four dimensional simplicial gravity*, preprint NBI-HE-94-29.
- [12] B. Brüggmann and E. Marinari, *More on the exponential bound of four dimensional simplicial quantum gravity*, MPI-PHT-94-72.
- [13] B.V. de Bakker and J. Smit, Phys. Lett. B334 (1994) 304.
- [14] F. David, Nucl. Phys. B368 (1992) 671.

- [15] M.E. Agishtein and A.A. Migdal, Nucl. Phys. B350 (1991) 690; N.K. Kawamoto, V.A. Kazakov, Y. Saeki and Y. Watabiki, Phys. Rev. Lett. 68 (1992) 2113; J. Ambjørn, P. Białas, Z. Burda, J. Jurkiewicz and B. Petersson, Phys. Lett. B342 (1995) 58.
- [16] T. Filk, Mod. Phys. Lett. A7 (1992) 2637.
- [17] H.W. Hamber, Nucl. Phys. B400 (1993) 347.
- [18] W. Beirl, E. Gerstenmayer, H. Markum and J. Riedler, Phys. Rev. D49 (1994) 5231.
- [19] B.V. de Bakker and J. Smit, Nucl. Phys. B (Proc. Suppl.) 34 (1994) 739.
- [20] M. Lüscher and P. Weisz, Phys. Lett. B212 (1988) 472; Nucl. Phys. B318 (1989) 705; U.M. Heller, Nucl. Phys. (Proc. Suppl.) 34 (1994) 101.
- [21] J. Frölich and T. Spencer, Comm. Math. Phys. 83 (1982) 411; V. Alessandrini, Nucl. Phys. B215 (1983) 337; V. Alessandrini and Ph. Boucaud, Nucl. Phys. B225 (1983) 303.